Characterization and modeling of the demagnetization processes in exchange-coupled $SmCo_5/Fe/SmCo_5$ trilayers

R. Pellicelli,[1] M. Solzi,[1] V. Neu,[2] K. Häfner,[2] C. Pernechele,[1] and M. Ghidini[1]
[1]*Dipartimento di Fisica e CNISM, Università di Parma, Via G. P. Usberti 7/A, 43100 Parma, Italy*
[2]*Institute for Metallic Materials, IFW Dresden, P.O. Box 270116, D-01171 Dresden, Germany*
(Received 22 December 2009; revised manuscript received 6 May 2010; published 24 May 2010)

The demagnetization processes in epitaxially grown $SmCo_5/Fe/SmCo_5$ trilayers have been analyzed in the framework of a one-dimensional micromagnetic model, exploiting the well-defined orientation of the easy magnetization axis present in both $SmCo_5$ layers. The applied magnetic field is considered along easy, hard, and tilted directions. For the case of hard direction, the nucleation field equation and the analytical expression of the critical susceptibility are given. Due to the observed separate switching behavior of the two hard layers in the realized trilayers, the analysis also considers demagnetization processes in which the two hard layers have opposite magnetic polarization. Calculations based on the nominal values of the magnetic and geometric parameters for the ideal symmetric trilayer are only in qualitative agreement with the corresponding experimental curves. In order to explain the discrepancies, the influence of variations in the parameters has been deeply analyzed, as well as the effect of a distribution of tilting angles of the hard layers anisotropy axes. In addition, we have extended the model to treat the case of a real asymmetric trilayer, characterized by slightly different anisotropy properties of the two hard layers, and we have derived the corresponding nucleation field equation for the case of easy direction. This analysis shows that a better agreement between calculations and measurements concerning the reversible behavior of the trilayers can be achieved by slightly modifying the nominal soft layer thickness and by assigning different tilting angles to the hard layers. Moreover, it shows that the remaining discrepancies can be ascribed to imperfections, which cannot be considered in detail in the one-dimensional model.

DOI: 10.1103/PhysRevB.81.184430 PACS number(s): 75.60.Jk, 75.60.Ej, 75.70.Cn

I. INTRODUCTION

The study and understanding of exchange coupling between hard and soft magnetic materials across their phase boundary benefit from well-defined geometrical and magnetic properties of the constituting phases. Especially, a unique orientation of the hard phase's easy axis allows a comparison of experimental data with calculations in a one-dimensional model, which assumes a uniform magnetization in planes parallel to the phase boundary and characterizes the coupled films with a spin spiral along the normal of the phase boundary. Consequently, hard/soft bilayers based on epitaxial hard magnetic Sm-Co thin films, which can be grown in a smooth and controlled fashion,[1,2] have been studied extensively for exchange-coupling effects. In an early work of Fullerton *et al.*,[3] both the longitudinal and transversal magnetization components in the demagnetizing branch of an epitaxial Sm-Co/Fe bilayer with field parallel to the easy axis could be modeled to satisfaction with a one-dimensional atomistic model. In subsequent works, the spin spiral has been experimentally determined with depth sensitive methods[4,5] on such structures. Recently, also hard/soft/hard trilayers have been prepared epitaxially, such that the easy axes of both hard layers are parallel.[6] These films are based on 25-nm-thick hard magnetic $SmCo_5$ layers with large uniaxial anisotropy and soft magnetic Fe of thickness 6 and 16 nm. They show exceptionally large energy densities due to the improved magnetic properties of the $SmCo_5$ layers and the presence of two coupling interfaces.

A previously described micromagnetic one-dimensional model[7] has been applied to carry out a thorough analysis of the demagnetization processes in the $SmCo_5/Fe/SmCo_5$ exchange-coupled trilayers, considering both easy and hard demagnetization curves and utilizing non-normalized values of magnetic polarization. Exchange-coupled systems[8] (also known as exchange-spring magnets[9]) show a peculiar two-stage magnetic polarization reversal, beginning at a well-defined critical field, the nucleation field, at which the magnetic moments start to deviate reversibly and nonuniformly from the easy direction, and followed by the reversal field that promotes the irreversible switching of the whole system. The analysis applied to multilayered planar systems for both parallel and perpendicular anisotropy reveals the presence of different reversal regimes.[7,10,11] The related phenomenology, once assigned the intrinsic properties of the materials, can be synthetically summarized in a magnetic phase diagram as a function of the individual layer thicknesses.[7] The diagrams have in principle a predictive potential on the behavior of any particular composite and therefore can be useful for tailoring the properties of these systems. For a trilayer system with identical $SmCo_5$ layers the geometry is symmetric with respect to the central Fe layer and so is the configuration of the spin spiral if the initial polarization state is also symmetric. In this work, the adopted one-dimensional model has been extended in order to also consider solutions in which the magnetic polarizations of the two hard layers have opposite directions. These configurations can be experimentally accessed in real trilayers because of the possible independent switching of the two hard layers.[6]

Because of the specific type and conditions of the growing process, real trilayers show a behavior that can slightly diverge from the ideal one. This difference can be due first of

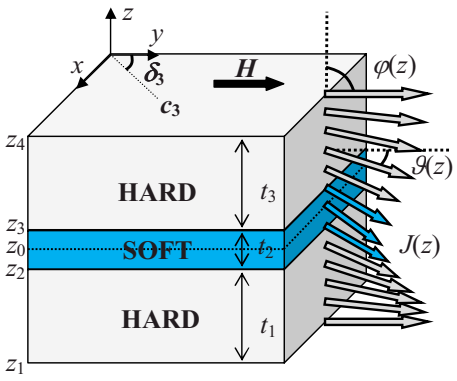

FIG. 1. (Color online) Basic scheme for the one-dimensional micromagnetic continuum model of the hard/soft/hard trilayer.

all to a nonperfect control over the nominal values of the magnetic and geometric parameters, and second to imperfections, which only partly can be taken into account in the ideal model. In particular, the calculations based on the nominal values of the parameters for the ideal symmetric $SmCo_5/Fe/SmCo_5$ trilayer show only a qualitative agreement with the experimental demagnetization curves for both the reversible and the irreversible portions. In order to explain the quantitative discrepancies in the reversible behavior of the trilayers, numerical simulations have been performed to deeply analyze the influence of variations in the parameters on the demagnetization process. Moreover, the one-dimensional model has been further developed to describe the behavior of asymmetric trilayers characterized by different anisotropy properties of the two hard layers, to the aim of taking into account asymmetries unavoidably present in real systems. This analysis also shows that the remaining discrepancies, which mainly concern the irreversible behavior, can be ascribed to imperfections of real trilayers, which cannot be considered in details in the one-dimensional model.

The paper is organized as follows. A general theoretical treatment of the demagnetization processes for the ideal $SmCo_5/Fe/SmCo_5$ trilayer is presented in Sec. II. In particular, the theoretical model is described in Sec. II A and solutions for the symmetric trilayer are discussed in Sec. II B. Section III reports a brief account of experimental details in Sec. III A and the application of the model to the realized trilayers in Sec. III B. Finally, Sec. IV deals with the theoretical analysis of the effect of the parameters variation (Sec. IV A) and the influence of asymmetries in the two hard layers (Sec. IV B) while the results of this analysis are applied to the experimental data in Sec. IV C.

II. MODELING OF THE DEMAGNETIZATION PROCESSES

A. Theoretical model

Let us consider a hard/soft/hard trilayer (see Fig. 1) with uniaxial magnetocrystalline anisotropy characterized by easy axes c_i and anisotropy constants K_i, where $i=1,2,3$ for the bottom hard, middle soft, and top hard layers, respectively. The demagnetization process can be in principle described by means of a one-dimensional model in which the magnetic polarization $J=\mu_0 M$ is uniform on the planes of the trilayer and thus it depends only on the perpendicular coordinate z while its direction is expressed by the azimuthal angle $\vartheta(z)$ and the polar angle $\varphi(z)$. The polarization vector inside each layer is subjected to the action of the torque exerted by the effective field H_{eff}, which is the negative functional derivative of the total magnetic Gibbs free energy.[12–14] The effective field is the sum of the exchange, anisotropy and demagnetizing fields, as well as of the external magnetic field H. Due to the uniformity of the polarization on the planes of the trilayer, the demagnetizing field is uniform on these planes and perpendicular to them, and its expression is $H_d=-J_i/\mu_0 \cos\varphi$,[15] where J_i is the saturation polarization. The exchange coupling at the interface between two layers can be described by introducing a torque per unit area $\vec{\tau}_{i-1,i}=-\vec{\tau}_{i,i-1}=2I_{i-1,i}\vec{j}(z_{i^-})\times\vec{j}(z_{i^+})$ $(i=2,3)$, where $\vec{j}$ is the polarization unit vector and $I_{i-1,i}$ is the intensity of the interface exchange interaction. Due to the vanishing of the exchange torque at the free surfaces and to the exchange-coupling torque at the interfaces, the polarization vector satisfies the following boundary conditions:

$$\left.\frac{d\vec{j}}{dz}\right|_{z_i}=0 \quad (i=1,4) \quad A_{i-1}\vec{j}(z_{i^-})\left.\frac{d\vec{j}}{dz}\right|_{z_{i^-}}$$

$$=A_i\vec{j}(z_{i^+})\left.\frac{d\vec{j}}{dz}\right|_{z_i^+}$$

$$=I_{i-1,i}\vec{j}(z_{i^-})\vec{j}(z_{i^+}) \quad (i=2,3), \tag{1}$$

where A_i is the exchange-stiffness constant. In the limit case of strong coupling[7] between the layers ($I_{i-1,i}\to\infty$, as it happens inside the layers according to the continuum micromagnetic theory), the boundary conditions at the interfaces imply that $\vec{j}(z_{i^-})\to\vec{j}(z_{i^+})$, which corresponds to a continuous variation in the polarization unit vector across the hard/soft interface.[7] The equilibrium condition $\vec{m}\times\vec{H}_{\text{eff}}=0$ allows deducing the Euler equation[13,16,17] for $\vartheta(z)$ and $\varphi(z)$. The solutions of the Euler equation that also satisfy the boundary conditions of Eq. (1) correspond to the equilibrium states of the polarization.

In the present treatment, unless advised otherwise, the easy axes c_i lie in the trilayer plane, the external field H is applied parallel to the y axis (see Fig. 1) and a strong interface coupling is assumed. The equilibrium solutions have been calculated by numerically integrating the related Landau-Lifschitz-Gilbert (LLG) equation[18] with a one-dimensional grid on the z axis.[15] In the case of strong interface exchange coupling, we have assumed $I_{i-1,i}=I_{\text{strong}}=A_{\text{strong}}/\Delta z$, where Δz is the vertical mesh width and A_{strong} is the mean of the exchange-stiffness constants assigned to the soft and hard layers.[15] All the performed simulations show that the angle φ vanishes when the system reaches an equilibrium state. This result corroborates the validity of the assumption $\varphi(z)=0$ supposed when the one-dimensional model is applied to multilayers with planar anisotropy,[16,19] even if a rigorous deduction of its validity only exists for the case of perpendicular anisotropy.[7] The above assumption has been adopted in all the analytical calculations performed in

the present analysis. The validity of the obtained results has also been verified by the direct numerical integration of the Euler equation [assuming $\varphi(z)=0$] with the shooting method.[20]

B. Symmetric trilayer

Let us consider now the particular case of a trilayer with identical hard layers ($t_1=t_3$, $A_1=A_3$, $K_1=K_3$, and $J_1=J_3$) and identical easy axis directions for the three layers ($c_1=c_2=c_3$). If the initial state of the system is the saturated one, the equilibrium solution $\vartheta(z)$ is an even function with respect to the central coordinate $z_0=z_2+t_2/2$. Thus, the analysis of the demagnetization process is performed on a half trilayer with the additional boundary condition $d\vec{j}/dz=0$ at $z=z_0$.

1. Field applied along the easy direction

If the external field H is applied along the easy positive direction ($\delta_i=0$), the demagnetization process is characterized by two critical fields,[17] which are defined as positive numbers even if they lie in the second quadrant of the H-J plane: (i) the nucleation field H_n, at which the magnetic moments start to deviate reversibly and nonuniformly from the easy direction; (ii) the reversal field $H_r \geq H_n$ that promotes the irreversible rotation of the whole system. The critical susceptibility $\chi_n=dJ/d(\mu_0 H)$ at the nucleation field[17] turns out to be a key parameter to describe the type of reversal process, as magnetic (saturation polarization, anisotropy, and exchange) and geometric (layer thicknesses) properties of the layers are varied. As a result, a general magnetic phase diagram, pointing out three different regimes of reversal is obtained in the layers thickness plane.[17] The rigid magnet (RM) regime is characterized by the coincidence of the two critical fields so that the hysteresis loop shows an irreversible sudden jump to inverse saturation. On the contrary, in the exchange-spring (ES) regime, the demagnetization curve includes a reversible portion between the two critical fields. The adopted one-dimensional model does not consider the role of domains and domain-wall nucleation and pinning in the xy plane. Hence, the obtained values of the reversal field should be considered as an upper limit for the real switching field H_{sw}, at which the irreversible phenomena related to nucleation and propagation of reversed domains take place. Figure 2 shows a significant region of the magnetic phase diagram (in the plane of the soft and hard layer thickness t_2 and t_3) for the symmetric trilayer $SmCo_5/Fe/SmCo_5$, assuming $A_2=2.8\times10^{-11}$ J/m, $J_2=2.1$ T, $A_1=A_3=1.2\times10^{-11}$ J/m, $K_1=K_3=10$ MJ/m^3, and $J_1=J_3=0.91$ T while the Fe layer anisotropy constant is assumed to be negligible ($K_2=0$ as for an ideal soft layer).

In the following we will illustrate the results of a series of simulations performed on a $SmCo_5/Fe/SmCo_5$ model trilayer with soft layer thickness $t_2=10$ nm and hard layer thickness $t_1=t_3=25$ nm. Figure 3(a) shows the demagnetization curve with the field applied along the easy axis direction (easy demagnetization curve): the two critical fields H_n and H_r, separated by the reversible portion of the curve (accordingly to the magnetic phase diagram of Fig. 2, where the considered trilayer lies in the ES region), are highlighted on the plot.

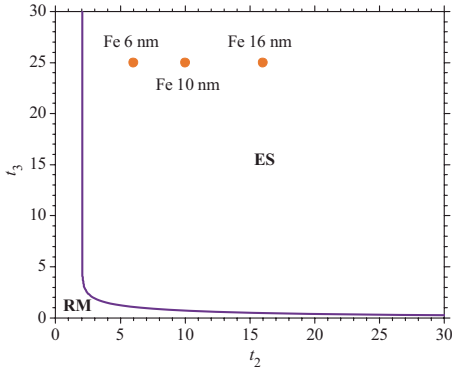

FIG. 2. (Color online) Magnetic phase diagram in the plane of layer thicknesses t_2 (soft) and t_3 (hard) for the $SmCo_5/Fe/SmCo_5$ symmetric trilayer. Representative points are evidenced, corresponding to different soft layer thicknesses (hard layer thickness $t_3=25$ nm).

2. Field applied along the hard direction

If the external field H is applied along the hard direction ($\delta_i=\pi/2$), the linearization of the Euler equation allows obtaining the implicit equation for the nucleation field H_n',

$$A_2\gamma_2 \tanh\left(\gamma_2\frac{t_2}{2}\right)=A_3\gamma_3\tan(\gamma_3 t_3), \tag{2}$$

where

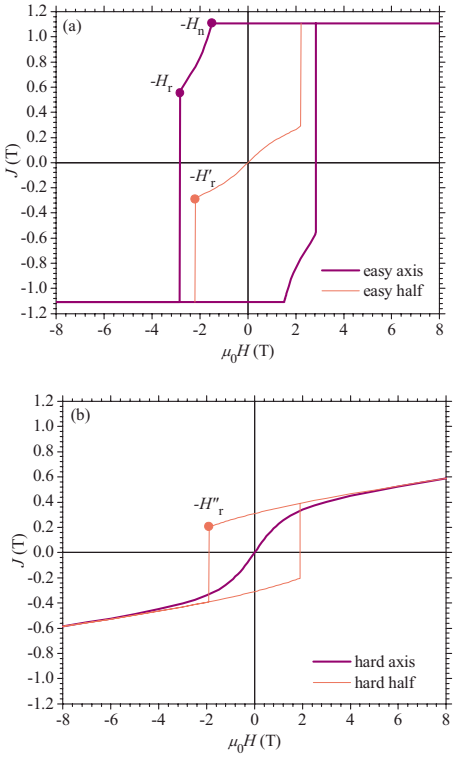

FIG. 3. (Color online) Simulated easy and hard demagnetization curves, and simulated easy and hard half-reversed solutions for the $SmCo_5/Fe/SmCo_5$ symmetric model trilayer. H_n: nucleation field, H_r, H_r', and H_r'': reversal fields.

$$\gamma_2 = \sqrt{-\left(\frac{K_2}{A_2} - \frac{J_2 H_n'}{2A_2}\right)} \quad \gamma_3 = \sqrt{\frac{K_3}{A_3} - \frac{J_3 H_n'}{2A_3}}.$$

The critical susceptibility χ_n' at the nucleation field can be deduced by expanding up to the fourth order in ϑ the expression of the derivative $d\vartheta/dz$ obtained starting from the first-order integral of the Euler equation, exactly as described in the treatment of Ref. 17 for the case of field applied along the easy direction. Thus, we obtain the expression

$$\chi_n' = \frac{J_2\left[\frac{t_2/2}{\cosh^2(\gamma_2 t_2/2)} + \frac{\tanh(\gamma_2 t_2/2)}{\gamma_2}\right] + J_3\left[\frac{t_3}{\cos^2(\gamma_3 t_3)} + \frac{\tan(\gamma_3 t_3)}{\gamma_3}\right]}{\frac{3p_2}{\cosh^2(\gamma_2 t_2/2)}\left[1 + \frac{\gamma_2 t_2}{\sinh(\gamma_2 t_2)}\right] - \frac{3p_3}{\cos^2(\gamma_3 t_3)}\left[1 + \frac{2t_3\gamma_3}{\sin(2\gamma_3 t_3)}\right] + 2(p_2 - p_3)}$$
$$\times \left\{\alpha_2\left[\frac{1}{\gamma_2^2} + \frac{t_2}{\gamma_2 \sinh(\gamma_2 t_2)}\right] + \alpha_3\left[\frac{1}{\gamma_3^2} + \frac{2t_3}{\gamma_3 \sin(2\gamma_3 t_3)}\right]\right\} \frac{1}{4\mu_0 H_n'(t_2/2 + t_3)}, \tag{3}$$

where

$$p_i = \frac{\alpha_i + 8\beta_i}{12(\alpha_i + 2\beta_i)} \quad \alpha_i = -\frac{J_i}{A_i} H_n' \quad \beta_i = \frac{K_i}{A_i} \quad (i = 2,3).$$

This expression is also valid in the case of a trilayer with perpendicular anisotropy (and field applied along the hard direction), if one performs the substitution $K_i \rightarrow K_i - J_i^2/(2\mu_0)$. Although it is in general possible to deduce a phase diagram also from Eq. (3) (for example, for multilayers with perpendicular anisotropy and field applied along the hard direction), however, in the case of planar anisotropy, the phase diagram is trivial as the critical susceptibility is always positive. In fact, the nucleation field [solution of Eq. (2)] turns out to lie in the first quadrant of the *H-J* plane, between the anisotropy field $2K_2/J_2$ of the soft layer and the anisotropy field $2K_3/J_3$ of the hard one. As a consequence it follows that $p_2 < 0$, $p_3 > 0$, and $\alpha_i < 0$ and thus $\chi_n' > 0$ so that the regime of the nucleation process is exclusively of exchange-spring type, according to the heuristic argument that the trilayer cannot reverse its polarization in the first quadrant. Moreover, when the applied field vanishes, the trilayer necessarily becomes fully saturated along the easy direction and thus the hard demagnetization curve crosses the origin of the *H-J* plane. Therefore, we conclude that the hard curve is fully reversible, to say without hysteresis, as reported in Fig. 3(b). This conclusion is confirmed by all the simulated hard demagnetization curves.

3. Half-reversed solutions

Since a real trilayer is never perfectly symmetric, it could happen that the two hard layers do not simultaneously switch during the demagnetization process.[6] As a consequence, a particular remanent magnetization state can be experimentally reached in which the two hard layers have opposite magnetization along the anisotropy axis (half-reversed remanent state). The corresponding $\vartheta(z)$ configuration is an odd function with respect to the central coordinate z_0 and, for symmetry reasons, it maintains such a property even under a field applied along the hard direction. Figure 3 shows the easy and hard simulated curves obtained starting from the half-reversed remanent state (half-reversed solutions) and considering the whole trilayer. In the case of the easy demagnetization curve, when the field reaches the reversal value $-H_r'$, the unreversed hard layer switches irreversibly as represented in Fig. 4(a). We find that this field is smaller in magnitude than the reversal field H_r from the fully saturated state, due to the fact that the spin spiral in the soft layer is twisted more strongly in the half-reversed solution. If the field is applied along the hard direction, the layer that irreversibly switches at the reversal field H_r'' is the soft one [see Fig. 4(b)], whereas the hard layer moments only rotate reversibly as in the case of even solutions. As a consequence, even and odd solutions merge above H_r''.

III. COMPARISON WITH THE EXPERIMENTAL DATA

A. Experimental details

The realized $SmCo_5/Fe/SmCo_5$ trilayers have been prepared by pulsed laser deposition under UHV conditions with nominally constant values of 25 nm for the two $SmCo_5$ layers and varying thickness of the soft Fe layer. Composition and layer resolved film thickness have been checked by energy dispersive x-ray analysis in combination with a thin-film analysis software.[21] Details on the preparation and characterization of the films are given in Ref. 6. Due the identical chemistry, the upper and lower $SmCo_5$ layer cannot be distinguished but rather a total thickness between 49 and 52 nm and an averaged composition of $Sm_{18}Co_{82}$ has been determined for all trilayers. As the ablation rates slightly reduce during the deposition process, for the identical preparation conditions (unchanged number of pulses on Sm and Co target) used in both layers, the second $SmCo_5$ layer is assumed to be somewhat thinner and enriched in Sm concentration, possibly leading to small differences in the switching behavior. Magnetization measurements have been performed in a physical properties measurement system with vibrating

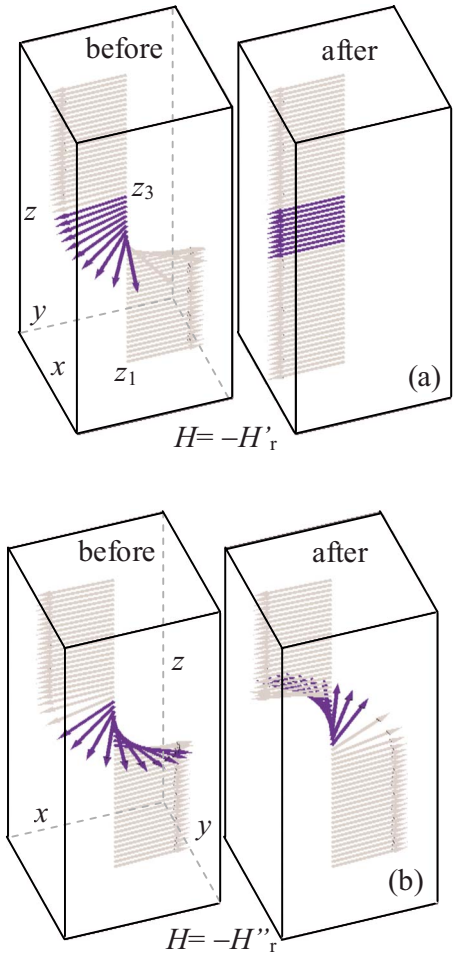

FIG. 4. (Color online) Simulated half-reversed solutions corresponding to the magnetic polarization configurations inside the $SmCo_5/Fe/SmCo_5$ symmetric model trilayer before and after: (a) the switching of the unreversed hard layer for the field applied along the easy direction and (b) the switching of the soft layer for the field applied along the hard direction.

sample magnetometer option in fields H up to 9 T. The saturation polarization of the $SmCo_5$ phase has been measured in the 50 nm $SmCo_5$ film by applying a 9 T magnetic field along the easy direction. Moreover, the uniaxial anisotropy constant has been deduced from the slope of the hard demagnetization curve for the same sample.

B. Application of the model

The previously described one-dimensional model has been applied to the experimental $SmCo_5/Fe/SmCo_5$ trilayers by assuming the same values reported in Sec. II for the constants J_i, A_i, and K_i. On the phase diagram of Fig. 2, two points representative of the trilayers with Fe thickness $t_2 = 6$ nm and $t_2 = 16$ nm are displayed. Both systems lie in the ES region and thus one would expect easy demagnetization curves with a reversible portion and two distinct critical fields, as actually verified in the simulated hysteresis loops reported in Fig. 5. However, the comparison with the experimental loops, reported on the same Fig. 5, shows a different

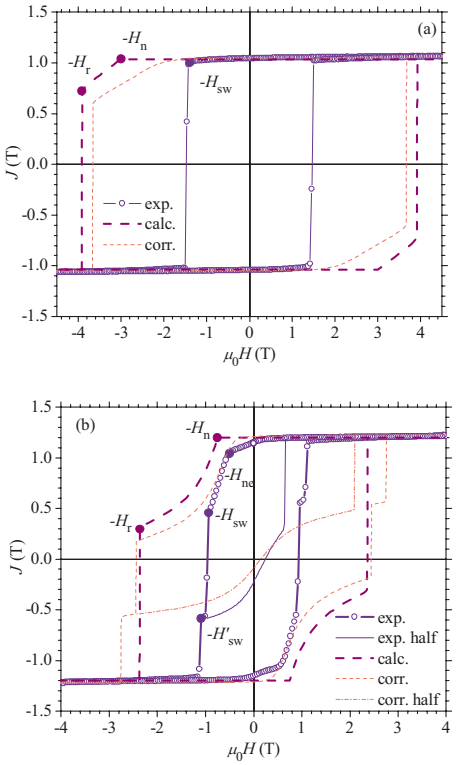

FIG. 5. (Color online) Comparison of simulated and experimental easy demagnetization curves for the $SmCo_5/Fe/SmCo_5$ trilayers with nominal soft layer thickness (a) $t_2 = 6$ nm and (b) $t_2 = 16$ nm. The simulated curves corrected assuming suitable values of the soft layer thickness and of the tilting angles (see text), are also displayed. In addition, (b) reports the experimental and the simulated-corrected magnetization curves obtained starting from the half-reversed remanent state. H_n and H_{ne}: nucleation fields; H_r: reversal field; and H_{sw} and H'_{sw}: switching fields.

behavior. In the case of $t_2 = 6$ nm, the reversible portion is not detectable probably because the system undergoes a sudden reversal due to domain nucleation and propagation occurring at a switching field $H_{sw} < H_n$ [see Fig. 5(a)]. In the case of $t_2 = 16$ nm, the reversible portion is evident (see also Ref. 6), although the experimental ($H_{ne} \cong 0.54$ T) and the calculated ($H_n = 0.75$ T) nucleation fields are slightly different, and also the experimental susceptibility is higher than the calculated one. Moreover, a reversible part with lower susceptibility is present in the experimental loop for fields $|H| < H_{ne}$ [see Fig. 5(b)].[6]

As expected, for both samples, the experimental switching fields result to be considerably lower than the calculated reversal fields. This is analogous to the typical behavior of single hard magnetic materials, where the coercive field is not as large as predicted from the anisotropy. In fact, the calculation of the reversal fields in the framework of the one-dimensional model is based on a criterion of instability of inhomogeneous rotation processes and the obtained values should be intended as an upper theoretical limit for the real switching fields, similar to the reversal field of the Stoner-Wohlfarth model with respect to the coercivity of real bulk magnets. The irreversible behavior in real systems is actually conditioned by the presence of domain walls nucleation and

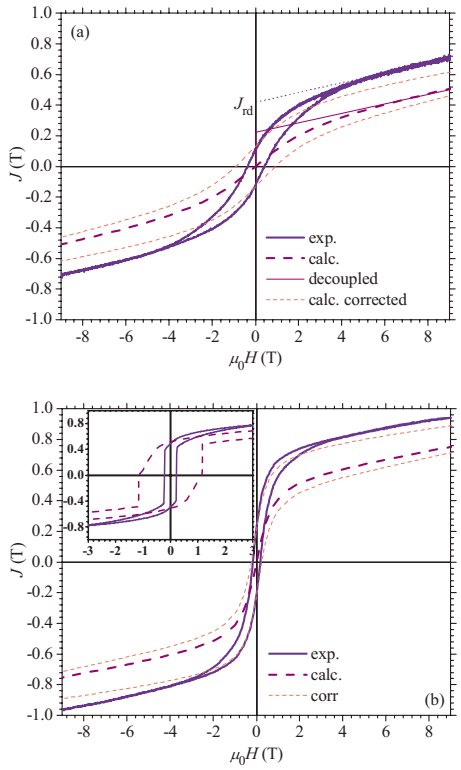

FIG. 6. (Color online) Comparison of simulated and experimental hard demagnetization curves for the $SmCo_5/Fe/SmCo_5$ trilayers with nominal soft layer thickness (a) $t_2=6$ nm and (b) $t_2=16$ nm. The simulated curves corrected assuming suitable values of the soft layer thickness and of the tilting angles (see text) are also displayed. In addition, the figures report (a) the simulated curve for the decoupled trilayer (J_{rd}: remanence of the extrapolated decoupled experimental curve) and (b inset) the experimental (dotted line) and simulated-corrected (dashed line) curves obtained starting from the half-reversed remanent state.

pinning. Moreover, the experimental curves are affected by magnetization relaxation phenomena[22] due to the slow dynamics and finite temperature of the measurement process. The irreversible switching of magnetization consequently occurs by overcoming energy barriers that separate the unreversed state from the reversed one. Therefore, the slower is the measurement process, the lower are the measured switching fields.[23] Still, the high uniaxial anisotropy of $SmCo_5$ ensures a large nucleation field which for the Fe 6 nm trilayer allows a square shaped hysteresis despite the large volume fraction of Fe. It has to be noted that for the Fe 16 nm sample, two different switching fields can be observed, which are probably related to the independent reversal of the hard layers ($H'_{sw} > H_{sw}$).[6] One can exploit this fact to also measure the half-reversed easy curve [see Fig. 5(b)]. An experimental remanent state that does not correspond to zero polarization ($J \cong -0.12$ T), proves that the trilayer is slightly asymmetric.

The experimental and calculated hard axis loops for the Fe 6 nm and 16 nm samples are shown in Fig. 6. Although a qualitative agreement between calculated and experimental curves is evident from Fig. 6, the experimental curves are clearly shifted toward larger absolute polarization values ($\Delta J \cong 0.2$ T for both trilayers). Moreover, the experimental curves show a small hysteresis that is not present in the simulated curves according to the discussion of Sec. II. The qualitative agreement between the calculated and experimental curves seems to confirm the presence of interface exchange coupling in the realized trilayers.

IV. INFLUENCE OF VARYING TRILAYER PARAMETERS

A. Symmetric trilayer

The details of the demagnetization process as well as the comparison between calculated and measured data strongly depend on both the magnetic (A_i, J_i, K_i) and geometric (t_i, δ_i) parameters of the trilayer. In the following, an analysis of their influence is performed on the basis of the one-dimensional model applied to the symmetric $SmCo_5/Fe/SmCo_5$ model trilayer.

1. Exchange-stiffness constant

In the previously described model a strong-type exchange coupling at the interface is assumed. However, one can release this hypothesis taking into account a reduced exchange coupling related to the possible presence of interface defects.[7,24] Consequently, in the case of the easy demagnetization curves, the nucleation field decreases while the reversal field increases. On the other hand, the susceptibility of the reversible portion of the curve turns out to be larger after the nucleation field and lower on reaching the reversal field because the demagnetization curve approaches that of the decoupled system. Thus the polarization before the reversal turns out to be always larger than $(2J_3t_3 - J_2t_2)/(2t_3 + t_2) = 0.4$ T. For the same reasons, when the field is applied in the hard direction, the effect of the reduced coupling is evident only at low fields, for which the initial susceptibility increases. The simulated easy and hard demagnetization curves corresponding to a case of weak interface coupling[7] with intensity $I_{i-1,i} = 0.05 \times I_{strong}$ are reported in Fig. 7. The considered weak character of the coupling allows the occurrence, in the easy curve, of a stable state characterized by a fully reversed soft layer and fully saturated hard layers above the critical field H_c, in agreement with the theoretical predictions.[7]

2. Layer thickness

In general, the layers thickness is affected by a certain amount of uncertainty with respect to nominal values due, for example, to the details of the growing process and to a possible phase intermixing at the hard/soft interfaces.[25] For hard layer thicknesses t_1 and t_3 considerably larger than the Bloch-wall width $d_i = 2\pi(A_i/K_i)^{1/2} \cong 7$ nm $(i=1,3)$, the hard layer thickness will not affect the critical-field values or even the coupling character according to the phase diagram of Fig. 2. On the other hand, changing the soft layer thickness directly influences nucleation and reversal fields for the considered thickness values. Both critical fields will decrease upon increasing the Fe layer thickness and a larger susceptibility is expected in the reversible portion of the easy demagnetization curve while the hard demagnetization curve shifts

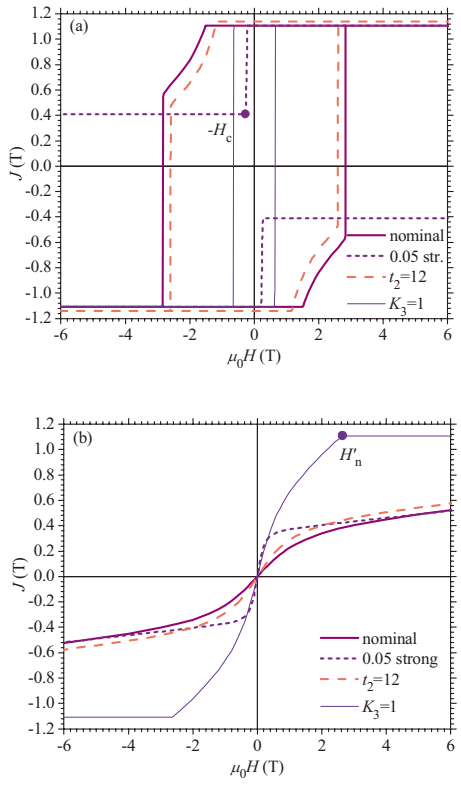

FIG. 7. (Color online) Simulated (a) easy and (b) hard demagnetization curves for the $SmCo_5/Fe/SmCo_5$ symmetric model trilayer, corresponding to: a reduced value $I_{i-1,i}=0.05\times I_{strong}$ of the interface exchange-coupling constant (dotted line); a reduced value $K_1=K_3=1$ MJ/m^3 of the hard layers anisotropy constant (solid thin line); an increased value $t_2=12$ nm of the soft layer thickness (dashed line). The above curves are compared to the nominal case $I_{i-1,i}=I_{strong}$, $K_1=K_3=10$ MJ/m^3, and $t_2=10$ nm (solid thick line). H_c: critical field and H'_n: nucleation field.

toward larger absolute values of the polarization. As regards the total saturation polarization of the trilayer $J_s=(2J_3t_3+J_2t_2)/(2t_3+t_2)$, it tends to increase both on enlarging the soft layer thickness and on reducing the hard layer one, with a more evident modification in the case of a change in the soft layer thickness. The simulated easy and hard demagnetization curves are reported in Fig. 7 for the case of 20% increment of the soft layer thickness with unchanged hard layer thickness.

3. Anisotropy constant

A possible uncertainty in the value of the anisotropy constant of the hard layers can have different causes. On the one hand, the considered constant is typically evaluated on a hard monolayer that in principle could be slightly different from the two hard layers of the trilayer. On the other hand the determination of the constant could be affected in itself by a large error since it is typically based on the extrapolation to high fields of the hard direction magnetization curve of the hard monolayer. In general, the value of K_1 directly determines the reversal and nucleation fields $H'_n=H_r=2K_1/J_s$ for a single $SmCo_5$ layer in the easy and hard directions, respectively, according to the simple Stoner-Wohlfarth theory, and the purely rotational hard axis curve will rise with a slope given by $J_s/H'_n\sim 1/K_1$. A similar effect is expected for the coupled trilayers. Therefore, for both easy and hard curves, all the critical fields turn out to be decreased and the susceptibility increased by reducing the value of K_1, as reported in Fig. 7 for $K_1=K_3=1$ MJ/m^3. The nucleation field $H'_n=2.65$ T deduced from Eq. (2) is evidenced on the hard demagnetization curve [see Fig. 7(b)] and it is coincident with that obtained from the simulated curve.

4. Anisotropy axis

So far, the model considers one single anisotropy axis and a well-defined field direction. In realistic samples, even epitaxial, well textured films will have a spatial distribution of easy axis orientations with respect to an average direction. Furthermore, the applied field direction with respect to the average direction of the anisotropy axes might not be perfectly accurate. In the framework of the one-dimensional model, both the above effects can be taken into account by simply introducing a tilting angle in the xy plane between the applied field direction and the average direction of the anisotropy axes. The simulated easy and hard demagnetization curves are reported in Fig. 8 for a tilting angle $\delta_1=\delta_3=10°$ in the xy plane. The easy-direction nucleation process turns out to be less sharp and it starts to become evident at lower absolute field values while the susceptibility of the reversible portion is smaller. On the contrary, the reversal field tends to shift to larger values. With reference to the hard demagnetization curve, the introduction of a tilting angle leads to the occurrence of a hysteresis, whose area increases for larger tilting angles, and of an irreversible switching (not shown in Fig. 8) for high absolute field values. Moreover, the two branches of the curve differ from the untilted curve by a vertical shift toward larger absolute values of the polarization. The possible occurrence of a tilting angle in the vertical yz plane has also been simulated for the same angle value reported above, obtaining results very similar to the case without tilting (see Fig. 8).

5. Tilting angle distribution

The adopted one-dimensional model could give rise to inaccurate results in the case of a spatial distribution of the anisotropy axes directions. If the scale length L on which this phenomenon takes place is smaller than the Bloch-wall width of the hard phase ($d_1=d_3\cong 7$ nm), no effect is expected because the hard layer polarization tends to align itself along the average anisotropy axes direction. If, on the contrary, the scale length L is larger than d_1, the alignment of the hard layer polarization is toward the local anisotropy axis while the soft layer polarization should have a more complex behavior depending on the ratio between scale length L and soft domain-wall width $d_2=2\pi[A_2/(0.5\times J_2^2/\mu_0)]^{1/2}\cong 25$ nm. In fact, one expects that, if $L<d_2$, the soft layer behaves like as the coupled hard layer were aligned along the average direction and that, if $L>d_2$, Néel domain walls inside the soft layer occur in the xy plane. As an illustrative example, we have simulated the model trilayer by means of the software package LLG micromagnetics simulator,[26]

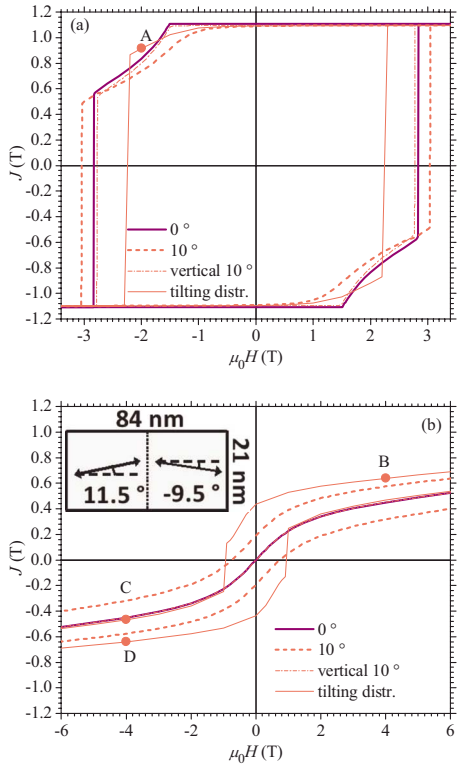

FIG. 8. (Color online) Simulated (a) easy and (b) hard demagnetization curves for the $SmCo_5/Fe/SmCo_5$ symmetric model trilayer, corresponding to different tilting angles of the hard layers anisotropy axes. The curves related to tilting angles 0° and 10° in the *xy* plane and 10° in the *yz* vertical plane have been obtained in the framework of the one-dimensional model while the curve corresponding to a spatial distribution of tilting angles has been simulated by utilizing the three-dimensional finite difference method. Inset: sketch of the tilting angle distribution of the hard layers inside the simulated region for the three-dimensional finite difference calculations.

which is based on the three-dimensional finite difference method.[12] We have assumed a simulation region of thickness 60 nm, with dimension 21×84 nm^2 and periodic boundary conditions in the *xy* plane [see inset of Fig. 8(b)]. In both hard layers, the anisotropy axis of a half trilayer is tilted by 11.5° while the tilting angle in the other half trilayer is −9.5° (tilting angles are set slightly different from ±10° to avoid spurious solutions), corresponding to a scale length $L = 42$ nm $> d_2$. The related easy and hard demagnetization curves (see Fig. 8) have been obtained by integrating the LLG equation with mesh size $1 \times 1 \times 1$ nm^3. The choice of this particular tilting angle distribution has been adopted in order to keep reasonably low the computation times: in fact, the needed integration time step of 10^{-14} s requires a computation time of about 1 s/step.

As regards the demagnetization process for the field applied along the easy direction, Fig. 9(a) reports a selected area of the simulated polarization configuration in the middle of the soft layer ($z = z_0$) for a field of −2 T [point A in Fig. 8(a)]: it is well evident the formation of a Néel domain wall in the *xy* plane. Accordingly, the susceptibility after the nucleation [see Fig. 8(a)] is lower than in the case of one-

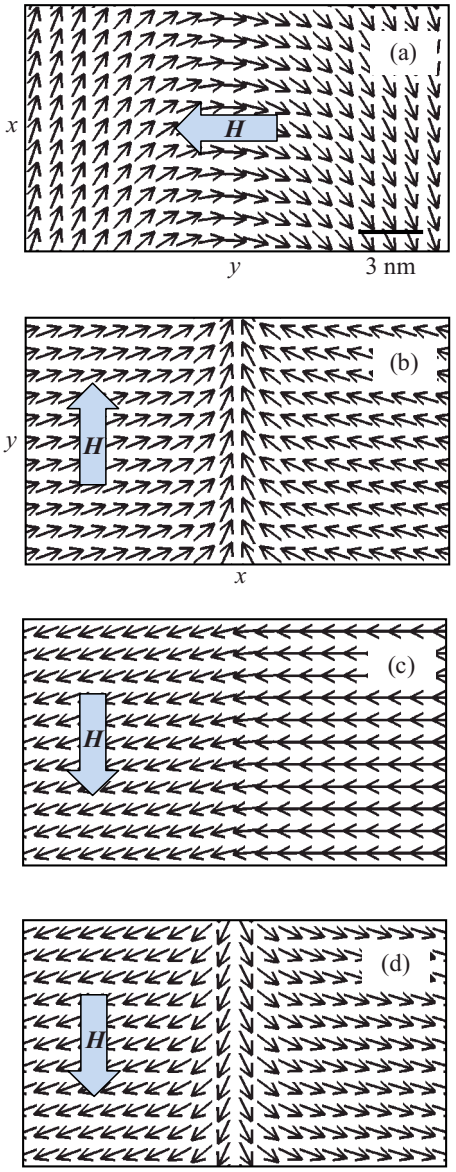

FIG. 9. (Color online) Selected areas of the simulated polarization configurations in the *xy* plane corresponding to the representative points of Fig. 8: (a) point A; (b) point B; (c): point C; and (d): point D.

dimensional tilting because the polarization in the soft wall is, on average, directed toward the saturated positive direction. Figure 8(a) also shows that the reversal field is lower than in the case of no tilting, contrary to the result obtained for the one-dimensional tilting.

The hard demagnetization curve [see Fig. 8(b)] is different from that obtained in the case of one-dimensional tilting: the polarization values are larger for positive fields while for intermediate values of negative fields, they are lower and almost coincident with those of the no-tilting case. This behavior can be understood if one considers the two typical polarization configurations of the hard layers for positive [point B in Fig. 8(b)] and negative [point C in Fig. 8(b)] applied field values, as reported in the selected areas of Figs. 9(b) and 9(c), respectively. In the positive case, the polarization directions inside the two tilted half regions are opposite

and a head-to-head domain wall[27] oriented parallel to the applied field is formed between the two half regions [tail-to-tail domain walls, not shown in Fig. 9(b), are formed at the left and right boundaries of the region]. On the contrary, in the negative case, the polarization directions inside the two half regions are parallel due to the irreversible switching of one half region. On further increasing the reversed applied field outside the range of Fig. 8(b), also the other half region switches irreversibly, causing the formation of a tail-to-tail domain wall in the center of the region: a similar polarization configuration, corresponding to point D [see Fig. 8(b)] in the return path of the hard hysteresis loop, is shown in Fig. 9(d).

The behavior of the trilayer considered in the above particular example is strongly influenced by the presence of domain walls in the *xy* plane of the system, as they extend over an area which corresponds (in the case of the soft layer) to 70% of the total film area. We are aware that real systems are much more complex than the above reported example. However, it is likely that the soft layer will nucleate toward the two opposite $\pm x$ directions in different points of the *xy* plane due to the presence of the tilting distribution. If the total area occupied by the domain walls is small with respect to film area, one expects that the trilayer behaves as the superposition of several one-dimensional contributions, which is equivalent, as regards reversible phenomena, to a system with an average one-dimensional tilting.

B. Asymmetric trilayer

When considering the fabrication of real trilayers, an unwanted but hardly avoidable effect is that the two nominally identical hard layers could present different properties, for example, because of the dissimilar growing conditions. We define here asymmetric trilayer a hard/soft/hard trilayer in which the two hard layers differ by the anisotropy constant and the tilting of the anisotropy axes. With particular reference to the realized $SmCo_5/Fe/SmCo_5$ trilayers (see Sec. III) one could hypothesize that the top $SmCo_5$ layer is characterized by a larger dispersion of the anisotropy constant values and/or of the tilting angles. In the following the effect of such asymmetry on the demagnetization curves will be treated. It is expected that the results of the simulations are substantially analogous to those obtained for the symmetric trilayer and that the asymmetry mainly affects the shape of the half-reversed curves. It is worth noting that the nucleation in the easy demagnetization curves remains a unique process, as in essence it only involves the soft layer (differently from what is expected in the case of an asymmetric soft/hard/soft trilayer). On the other hand, the reversal process, which mainly involves the hard layers, may occur as two separated switching events.

1. Anisotropy constant

We discuss the case in which the two hard layers are characterized by different values of the anisotropy constant, with the condition $K_3 < K_1$. The linearization of the Euler equation allows obtaining the implicit equation of the nucleation field H_n for the easy demagnetization curve,

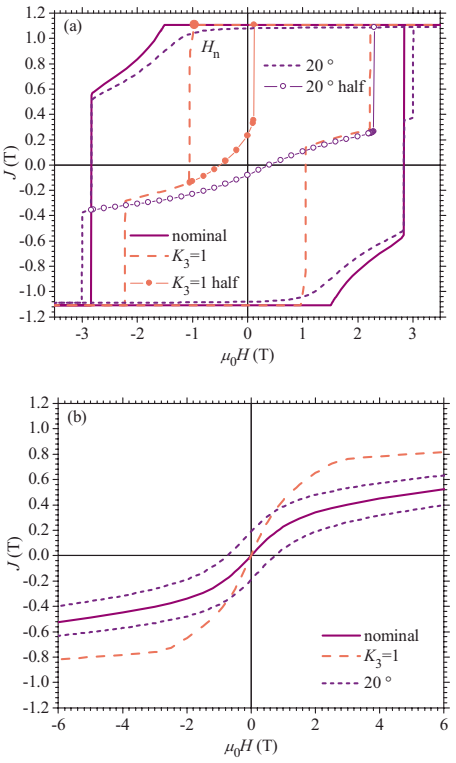

FIG. 10. (Color online) Simulated (a) easy and (b) hard demagnetization curves for the $SmCo_5/Fe/SmCo_5$ asymmetric model trilayer, corresponding to: a reduced anisotropy constant $K_3 = 1$ MJ/m^3 (dashed line) and a tilting angle $\delta_3 = 20°$ (dotted line) of the top hard layer. The above curves are compared to the nominal case $K_3 = 10$ MJ/m^3 and $\delta_3 = 0°$ (solid line). The corresponding easy magnetization curves simulated starting from the half-reversed remanent state are also displayed (lines with circles). H_n: nucleation field.

$$A_2\gamma_2[A_1\gamma_1 \tanh(\gamma_1 t_1) + A_3\gamma_3 \tanh(\gamma_3 t_3)] = [A_2^2\gamma_2^2 - A_1\gamma_1 A_3\gamma_3 \tanh(\gamma_1 t_1)\tanh(\gamma_3 t_3)]\tan(\gamma_2 t_2), \quad (4)$$

where

$$\gamma_1 = \sqrt{\frac{K_1}{A_1} - \frac{J_1 H_n}{2A_1}} \qquad \gamma_2 = \sqrt{-\left(\frac{K_2}{A_2} - \frac{J_2 H_n}{2A_2}\right)}$$

$$\gamma_3 = \sqrt{\frac{K_3}{A_3} - \frac{J_3 H_n}{2A_3}}.$$

The simulated easy and hard demagnetization curves are reported in Fig. 10 for a reduced anisotropy constant $K_3 = 1$ MJ/m^3 (without modifying the K_1 value). In the easy curve [see Fig. 10(a)], one can notice that, for the considered K_3 value, the top hard layer switches independently of the bottom one, thus allowing the half-reversed remanent state. In Fig. 10(a) it is also displayed the half-reversed easy curve obtained starting from this particular state: due to the asymmetry of the trilayer, this curve is remarkably asymmetric, with, in particular, a positive remanent polarization. The nucleation field $H_n = 0.96$ T deduced from Eq. (4) is evi-

denced on the easy curve and it is coincident with that obtained from the simulated curve. The hard demagnetization curve [see Fig. 10(b)] shows in general three different portions, each corresponding to the predominant demagnetization of a single layer.

2. Anisotropy axis

For the following the anisotropy constants of both layers are again taken to be identical ($K_1=K_3=10$ MJ/m^3) and we treat here the case of tilting of the anisotropy axis only in the top hard layer. The results of the simulations are reported in Fig. 10 for a tilting angle $\delta_3=20°$. A significant conclusion can be drawn from the simulation of the easy demagnetization curve in which the untilted hard layer switches before and independently of the tilted one. This result is in agreement with the expected larger value of the switching field for tilted layers (see, for example, the 1/cos Kondorsky's dependence of the switching fields[28] and experimental data on single $SmCo_5$ films[29]). It has also to be noticed that, as a consequence of this behavior, the half-reversed remanent state has a negative polarization [see the half-reversed easy curve in Fig. 10(a)].

C. Application to the realized trilayers

If one considers the one-dimensional analysis carried out in the previous parts of this section, it can be excluded that the disagreement between the experimental and simulated hard curves of Sec. III is caused by uncertainties of the exchange-stiffness constants or of the hard layers anisotropy constant. In fact, as regards the reduction in the exchange constant both inside the layers and at the interface, the corresponding demagnetization curves should tend, for high-field values, toward the curve of the decoupled trilayer [see, for example, the calculated decoupled curve in Fig. 6(a)]. Concerning the hard layers anisotropy constant, a reduction in its value determines an increase not only of the absolute polarization values but also of the susceptibility. Therefore, the above discrepancy can only be justified, in the framework of the one-dimensional model, by considering the uncertainties of the soft layer thickness and of the hard layer anisotropy axes directions (tilting). Indeed, an underestimated value of the soft layer thickness, including the possible occurrence of intermixing regions,[25] causes reduced values of the polarization. However, this reason cannot completely justify the observed differences. Actually, by linearly extrapolating the high-field values portion of the experimental curves toward zero-field values, one obtains that the intersection J_{rd} with the vertical axis corresponds to excessively high values of saturation polarization for the soft phase ($J_{rd}\cong 0.4$ T and $J_{rd}\cong 0.7$ T corresponding to $t_2=10.6$ nm and $t_2=22$ nm for the Fe 6 nm and 16 nm trilayers, respectively). Moreover, a too large increment of the soft phase thickness gives rise to overall saturation polarization values J_s larger than the experimental ones, as well as to excessively small values of the critical fields. Therefore, one also needs to assume the presence of a tilting angle between the hard phase anisotropy axes and the direction of the applied field. The estimate of the tilting angles obtained by using the slope of the nearly saturated portion of the easy demagnetization curves provides values ($\delta\geq 13°$ for the $SmCo_5$ film, $\delta\geq 15°$ for the Fe 6 nm trilayer, and $\delta\geq 20°$ for the Fe 16 nm trilayer) which are larger than those measured by different methods.[30] However, this estimate is probably affected by an overcompensation of the signal of the sample substrate, which is a further possible contribution to the observed discrepancy. Finally, a spatial distribution of tilting angles can be a further factor that determines an increment of the polarization in the hard demagnetization curves as well as a distribution of negative switching fields, as evidenced in Sec. IV A 5 of this section.

The simulated easy and hard demagnetization curves for the Fe 6 nm trilayer, corrected assuming soft layer thickness $t_2=7$ nm (with unchanged total thickness $t_2+2t_3=56$ nm) and tilting angles $\delta_1=\delta_3=7°$, are reported as an example in Figs. 5(a) and 6(a). The larger hysteresis present in the corrected hard curve is explained by the broad distribution of negative switching fields, which rules the reversal of polarization for negative fields in the experimental curve. Moreover, this curve is actually a minor loop, as the saturation is never achieved.

The simulated easy and hard demagnetization curves of the Fe 16 nm trilayer, corrected assuming a soft layer thickness $t_2=18$ nm (with unchanged total thickness $t_2+2t_3=60$ nm) and tilting angles $\delta_1=5°$ and $\delta_3=15°$, are reported as an example in Figs. 5(b) and 6(b). The choice of tilting angles $\delta_1\neq\delta_3$ has been suggested by the appreciable negative remanence of the experimental half-reversed easy curve. In the case of the simulated easy demagnetization curve, one can emphasize that the untilted hard layer reverses its polarization independently of the tilted one and for lower absolute field values. Also shown is the corresponding simulated half-reversed curve, which presents a negative remanent polarization like as the experimental one [see Fig. 5(b)].

Concerning the experimental easy demagnetization curve [see Fig. 5(b)], the presence of two adjacent distinct reversible portions cannot be justified in the framework of the one-dimensional model in which the reversible demagnetization is essentially a unique process (see Sec. IV B of this section). Thus, it is likely that a small portion of the trilayer has different magnetic properties.

The experimental and simulated curves obtained starting from the half-reversed remanent state for the case of field applied in the hard direction are also reported in the inset of Fig. 6(b). The curves have similar shapes, even if, as expected, the experimental one shows a lower switching field. In particular, also the experimental curve has a residual hysteresis after the occurrence of an abrupt switching, which can be ascribed to the abrupt reversal of the soft phase.

V. CONCLUSIONS

A one-dimensional micromagnetic theoretical model has been applied to the study of the demagnetization processes in $SmCo_5/Fe/SmCo_5$ trilayers. The model has been extended to also consider solutions of the symmetric trilayer in which the two hard layers have opposite magnetic polarizations. The numerical simulations applied to a series of

$SmCo_5/Fe/SmCo_5$ realized trilayers and based on the nominal values of the parameters are only in qualitative agreement with the experimental demagnetization curves for both the reversible and the irreversible portions. Therefore, a thorough analysis of the influence of variations in the magnetic and geometrical parameters has been performed with reference to a $SmCo_5/Fe/SmCo_5$ model system. Small asymmetric properties of real trilayers have also been considered in the model. Based on this analysis, the quantitative differences have been justified on the basis of uncertainties of the parameters as well as of irreversible phenomena and imperfections that can be considered only to some extent by the adopted theoretical treatment. In particular, we have verified that the differences concerning the reversible behavior of the trilayers can be reduced by introducing small changes in the soft layer thickness and by including different tilting of the anisotropy axes of the two hard layers. We have also shown that the remaining discrepancies, which mainly concern the irreversible behavior of the trilayers, could be partly due to a spatial distribution of tilting angles inside the layers. The performed analysis proves that the one-dimensional model can be helpful for a better understanding of exchange-coupled layered nanocomposites.

[1] E. E. Fullerton, J. S. Jiang, C. Rehm, C. H. Sowers, S. D. Bader, J. B. Patel, and X. Z. Wu, Appl. Phys. Lett. **71**, 1579 (1997).

[2] A. Singh, V. Neu, R. Tamm, K. Rao, S. Fähler, W. Skrotzki, L. Schultz, and B. Holzapfel, J. Appl. Phys. **99**, 08E917 (2006).

[3] E. E. Fullerton, J. S. Jiang, M. Grimsditch, C. H. Sowers, and S. D. Bader, Phys. Rev. B **58**, 12193 (1998).

[4] V. E. Kuncser, M. Doi, W. Keune, M. Askin, H. Spies, J. S. Jiang, A. Inomata, and S. D. Bader, Phys. Rev. B **68**, 064416 (2003).

[5] Y. Choi, J. S. Jiang, J. E. Pearson, S. D. Bader, J. J. Kavich, J. W. Freeland, and J. P. Liu, Appl. Phys. Lett. **91**, 072509 (2007).

[6] V. Neu, K. Häfner, A. K. Patra, and L. Schultz, J. Phys. D **39**, 5116 (2006).

[7] G. Asti, M. Ghidini, R. Pellicelli, C. Pernechele, M. Solzi, F. Albertini, F. Casoli, S. Fabbrici, and L. Pareti, Phys. Rev. B **73**, 094406 (2006).

[8] R. H. Victora and X. Shen, IEEE Trans. Magn. **41**, 537 (2005).

[9] E. F. Kneller and R. Hawig, IEEE Trans. Magn. **27**, 3588 (1991).

[10] M. Ghidini, G. Asti, R. Pellicelli, C. Pernechele, and M. Solzi, J. Magn. Magn. Mater. **316**, 159 (2007).

[11] G. P. Zhao, X. L. Wang, C. Yang, L. H. Xie, and G. Zhou, J. Appl. Phys. **101**, 09K102 (2007).

[12] J. Fidler and T. Schrefl, J. Phys. D **33**, R135 (2000).

[13] M. Solzi, C. Pernechele, R. Pellicelli, M. Ghidini, F. Albertini, and C. Casoli, J. Magn. Magn. Mater. **316**, e313 (2007).

[14] V. Dubuget, A. Thiaville, F. Duverger, S. Dubourg, O. Acher, and A. L. Adenot-Engelvin, Phys. Rev. B **80**, 134412 (2009).

[15] M. Grimsditch, R. Camley, E. E. Fullerton, S. Jiang, S. D. Bader, and C. H. Sowers, J. Appl. Phys. **85**, 5901 (1999).

[16] T. Leineweber and H. Kronmüller, J. Magn. Magn. Mater. **176**, 145 (1997).

[17] G. Asti, M. Solzi, M. Ghidini, and F. M. Neri, Phys. Rev. B **69**, 174401 (2004).

[18] D. Suess, V. Tsiantos, T. Schrefl, J. Fidler, W. Scholz, H. Forster, R. Dittrich, and J. J. Miles, J. Magn. Magn. Mater. **248**, 298 (2002).

[19] E. Goto, N. Hayashi, T. Miyashita, and K. Nakagawa, J. Appl. Phys. **36**, 2951 (1965).

[20] W. H. Press, S. A. Teukolsky, W. T. Vetterling, and B. P. Flannery, *Numerical Recipes: The Art of Scientific Computing*, 3rd ed. (Cambridge University Press, Cambridge, 2007), Chap. 18.

[21] V. Neu, S. Fähler, A. Singh, A. R. Kwon, A. K. Patra, U. Wolff, K. Häfner, B. Holzapfel, and L. Schultz, J. Iron Steel Res. Int. **13**, 102 (2006).

[22] G. Bertotti, *Hysteresis in Magnetism* (Academic Press, San Diego, 1998).

[23] M. P. Sharrock, J. Appl. Phys. **76**, 6413 (1994).

[24] K. Yu. Guslienko, O. Chubykalo-Fesenko, O. Mryasov, R. Chantrell, and D. Weller, Phys. Rev. B **70**, 104405 (2004).

[25] Y. Choi, J. S. Jiang, Y. Ding, R. A. Rosenberg, J. E. Pearson, S. D. Bader, A. Zambano, M. Murakami, I. Takeuchi, Z. L. Wang, and J. P. Liu, Phys. Rev. B **75**, 104432 (2007).

[26] http://llgmicro.home.mindspring.com/

[27] M. Kläui, J. Phys.: Condens. Matter **20**, 313001 (2008).

[28] E. Kondorsky, J. Phys. (USSR) **2**, 161 (1940).

[29] A. Singh, V. Neu, S. Fähler, K. Nenkov, L. Schultz, and B. Holzapfel, Phys. Rev. B **77**, 104443 (2008).

[30] A. Singh, V. Neu, S. Fähler, K. Nenkov, L. Schultz, and B. Holzapfel, Phys. Rev. B **79**, 214401 (2009).